Master of Science dissertation:

Evaluation of accuracy in simultaneous dual-radionuclide activity quantification in preclinical instruments – scintillation counter, digital autoradiography and micro-SPECT/CT

Jonas Ahlstedt

Supervisors:

Anders Örbom
Thuy Tran
Sven-Erik Strand

Department of Medical Radiation Physics, Clinical Sciences, Lund
Lund University, Sweden, 2011

Abstract

Introduction: The development and optimization of methods for multi-radionuclide measurements in preclinical *in vivo* and *ex vivo* SPECT imaging could potentially improve studies in which more than one pharmaceutical is being investigated. The aim of this study is to quantitatively compare and evaluate different methods for these types of measurements using three different modalities – a small animal SPECT/CT, a scintillation counter and a digital autoradiography instrument. This work will also investigate the possibilities of performing a multi-radionuclide study in practice through an animal pilot study.

Materials and methods: Phantom measurements were performed on all three instruments, comparing their ability to quantify activity when a single radionuclide is measured in contrast to when two radionuclides are used. For these purposes, the two radionuclides ^{99mT}Tc and ^{111}In were used. For the animal pilot study, the HER2-targeting Affibody and Trastuzumab were labeled with ^{99m}Tc and ^{111}In respectively. Ten NMRI mice (male and female) were injected with ^{99mT}Tc -Affibody and ^{111}In-trastuzumab and imaged using a small animal SPECT/CT camera. Scintillation counting and digital autoradiography were used to measure and/or image the activity in excised organs.

Results: Differences between single and dual-radionuclide measurements was about 5 % for the scintillation counter and the small animal SPECT/CT system. The same holds for the digital autoradiography system, except for low statistics where ^{99m}Tc was overestimated. Phantom measurements also suggest that correction factors could be calculated, if more data was acquired. In the animal pilot study, all imaging cameras in the study managed to visualize and quantify both radiotracers using dual-radionuclide protocols.

Conclusions: This study has shown the possibility to perform quantitative dual-radionuclide measurements on all systems used in this study. Results from the phantom studies suggest that corrections for instrument dead-time and crosstalk could be made. More data is needed in order to calculate such correction factors accurately following the protocols suggested in this study.

Att titta på två radionuklider samtidig – en utvärdering av olika detektorsystem

Målet med detta examensarbete är att undersöka hur bra olika kamerasystem och detektorer som används inom preklinisk forskning kan mäta på två radionuklider samtidigt. Att kunna mäta på två radionuklider samtidigt skulle kunna förbättra djurstudier där man undersöker två mediciner samtidigt eftersom det blir möjligt att undersöka båda medicinerna i samma djur. Detta minskar felet som kommer av de individuella reaktionerna på medicinen samtidigt som det minskar behovet av antalet djur vilket gör metoden intressant både ur ett statistiskt, ekonomiskt och etiskt perspektiv. I denna studie undersöks de två molekylerna Trastuzumab och Affibody. Båda molekylerna delar egenskapen att de söker sig till och fastnar på samma typ av receptor-molekyl. Denna receptor-molekyl kallas för HER2-receptorn som är vanligt förekommande i bröstcancertumörer hos kvinnor. För att kunna se hur dessa molekyler sprider sig i ett försöksdjur så tar man bilder med olika detektorsystem. För att detektorsystemen ska kunna se vart molekylerna befinner sig fäster man radioaktiva isotoper, eller radionuklider, på molekylerna. När dessa radionuklider sönderfaller skickar de ut beta- och gammastrålning som detekteras av detektorsystemen. Radionukliderna som användes i detta försök var Indium-111 och Technetium-99m, där Trastuzumab var märkt med Indium-111 och Affibody med Technetium-99m. Tre stycken detektorsystem utvärderades: en SPECT-kamera (Single Photon Emission Computed Tomography), ett provväxlarsystem, samt ett autoradiografi-instrument. Med SPECT-kameran kan man se hur molekylerna har fördelat sig i hela djuret på organnivå. Man kan också ta flera bilder på samma djur med olika tidsintervall och på så sätt få en uppfattning om hur fördelningen ändras över tiden. Provväxlarsystemet kan mäta hur mycket av molekylerna som finns i varje organ, men inte ta några bilder. Fördelen med provväxlaren är att den kan mäta mycket låga halter av molekylerna. Med autoradiografisystemet kan man se fördelningen med en mycket hög upplösning i enskilda organ. För att få en fullständig bild av fördelningen behövs alltså alla tre instrumenten. För att man ska kunna mäta på två olika radionuklider samtidigt utnyttjas några av de olika egenskaperna radionukliderna har, som till exempel halveringstid och energi på utskickad strålning. För att utvärdera systemen på ett kvantitativt sätt jämfördes deras förmåga att mäta på enskilda radionuklider med mätsituationer där två radionuklider mättes samtidigt. Skillnaden mellan de båda mätsituationerna var ungefär 5 %. Resultaten visade att det är möjligt att utföra mätningar på två radionuklider samtidigt på samtliga instrument som ingick i studien. Resultat från ytterligare mätningar som gjordes visar på att korrektioner skulle kunna göras vilket skulle kunna ge ännu bättre resultat.

Table of contents

1 Introduction

Recent advancements in the field of preclinical imaging have provided researchers with dedicated small animal SPECT/CT, PET and MRI systems capable of monitoring biological processes in mouse and rat models with improved accuracy [1-3]. Prior to the advent of these innovations, radionuclide assays of animal models relied solely on clinical systems or techniques such as scintillation counting and autoradiography. While these techniques have advantages- such as high spatial resolution in the case of autoradiography and high sensitivity with scintillation counting- the non-invasive nature of the in vivo systems makes it possible to monitor biological processes in the same animal over time. In preclinical cancer research, the combined use of traditional and novel modalities can be used to study the distribution of a radiolabelled tumor-targeting pharmaceutical over time and at different levels of spatial resolution. To not only study the biodistribution with scintillation counting, but also with high resolution SPECT and autoradiography, is especially important from a dosimetric aspect, since distribution of activity in tissues/organs is rarely homogenous, something that is assumed in most dosimetric models [4].

In preclinical sciences a common type of study is one which is comparative; established pharmaceuticals, the effects of which are well documented, are compared to newer ones. Due to the biological variations between individuals, large groups of animals are required in these kinds of studies. This can be problematic for both practical and economic reasons, as well as controversial from an ethical perspective, and a reduction in the number of animals would be preferable. One possible way in which to reduce sample size is to compare both pharmaceuticals in the same animal at the same time. Previous studies have demonstrated that multi-radionuclide imaging with small-animal SPECT or PET is a promising method for quantitative measurement of several radionuclides [5, 6]. However, a more complete evaluation of these methods, employing SPECT, digital autoradiography and scintillation counting in one single quantitative study, has yet to be performed.

Trastuzumab (Herceptin®, Roche) is a humanized monoclonal antibody that targets the HER2-receptor which is overexpressed in a number of carcinomas, including breast carcinoma. Trastuzumab is used for treatment of breast cancer showing an overexpression of the HER2 protein. To this date, three different methods for the evaluation of HER2-status are approved by the U.S. Food and Drug Administration (FDA) [7]. All these methods are invasive; biopsies from patients are analyzed either through immunohistochemistry (IHC), fluorescence *in situ* hybridization (FISH) or chromogenic *in situ* hybridization (CISH). Unlike a biopsy, the assessment of HER2-status through molecular imaging could potentially provide a non-invasive method capable of monitoring the entire expression of HER2 in a single scan as well as determining HER2-status of both the primary tumor and metastases. The development of a tracer that has a high affinity for the HER2-receptor and yields high contrast is therefore desirable.

One molecule that does display such properties is the HER2-binding Affibody, the small size of which yields characteristics such as rapid kinetics and high tumor/blood ratio. Diagnostic imaging with Affibody, with its small size and high affinity for HER2, could therefore prove to be a better candidate than trastuzumab. Assessing HER2-status with imaging using trastuzumab or Affibody has been investigated before, with trastuzumab currently undergoing clinical trials [8-10]. However, comparing them quantitatively can be difficult because of the differences in methodology in each study and different animal models. Trastuzumab and Affibody are clearly suitable candidates for a multi-radionuclide measurement.

The development and optimization of methods for multi-radionuclide measurements in small-animal SPECT imaging could potentially improve preclinical studies in which more than one pharmaceutical is being investigated. The aim of this study is to quantitatively compare and evaluate different measurement protocols for these types of measurements. This will be done for three different instruments: a small animal SPECT/CT imaging system, a digital autoradiography instrument and a scintillation counter. The experiments will be carried out through a series of phantom measurements as well as a pilot animal study. In the phantom measurements, ^{99m}Tc and ^{111}In will be used to evaluate each instrument. For the pilot animal study, the two targeting proteins Affibody and trastuzumab labeled with ^{99m}Tc and ^{111}In respectively will be used. The aim of the animal pilot study is to investigate the possibilities of performing a preclinical dual-radionuclide imaging study using the imaging systems mentioned above.

2   Background and theory

2.1   Small animal imaging

Before the transfer into clinical practice, new pharmaceuticals undergo extensive assessment processes. Animal models play an integral part in the preclinical stage, in which several imaging techniques have many different uses that range from drug discovery and evaluation to studying neurological, cardiovascular and oncological applications [3, 11]. Clinical imaging modalities, such as single photon emission computed tomography (SPECT), positron emission tomography (PET) or magnetic resonance imaging (MRI), have all undergone recent, significant improvements such as in increased efficiency and spatial resolution and exists in specialized versions as micro-SPECT, micro-PET and micro-MRI dedicated to preclinical research [12]. Many modern small animal SPECT and PET imaging systems also utilizes a computed tomography system (CT) and are capable of co-registering the x-ray images with the SPECT and PET images, providing an anatomical context as well as attenuation- and scatter corrections. The preclinical versions of these modalities have significantly higher spatial resolution then their clinical counterparts; spatial resolution for small animal SPECT and MRI are both at sub millimeter range. Small animal SPECT have the advantage of having many available radionuclides with appropriate energies and more convenient half-lives (^{99m}Tc, ^{111}In and ^{125}I) that are all easily produced. In contrast, small animal PET mainly utilizes radionuclides characterized by short half-lives (^{18}F, ^{11}C and ^{13}N), requiring a nearby cyclotron for the production. Although PET has superior efficiency (due to the lack of collimators) SPECT has seen great improvement in both efficiency and spatial resolution these areas over the past 15 years with optimized collimator design and the introduction of multi-pinhole systems [11].

An important concept in the field of preclinical imaging is the biomarker, which can be defined as a quantifiable, biological indicator of either a normal or a pathogenic process [13]. Once a biomarker is identified, the specific expression of the biomarker in the organism can be studied with the help of a radiotracer or a contrast agent. A radiotracer, or a radiolabeled tracer, is a molecule attached to a radioactive nuclide and that displays affinity for the biomarker. The emissions from the radiotracer are detected by an imaging system such as SPECT or PET. These images can be quantified and used to study biodistribution or the progression of tumor growth, with results eventually being extrapolated from the *in vitro* stage onto clinical trials and practice.

2.2 The HER2-receptor

The biomarker in this study is the human epidermal growth factor receptor 2 (HER2), a surface bound receptor tyrosine kinase[1]. It plays an important role in an array of cellular processes, including cell proliferation and apoptosis, and is one of four members in the EGFR-family [14]. An overexpression of the HER2 receptor, stemming from an amplification of the HER2-gene, occurs in 15-25 % of human breast cancers and is associated with a poor clinical prognosis as well as a more aggressive tumor growth [15-17]. Patients with an overexpression have a significantly lower survival rate and relapse time than those without [18]. In normal tissue however, the HER2-receptor is expressed only at very low levels, creating both a therapeutic and diagnostic window [17]. Radiotracer based imaging could potentially be used for the latter, creating a non-invasive, more effective alternative to the HER2-assessment techniques used today.

2.3 Targeting proteins

In this study the two targeting proteins trastuzumab and Affibody, both of which targets the HER2-receptor, will be labeled with ^{111}In and ^{99m}Tc and studied in a mouse model.

Trastuzumab

Breast cancer patients with an overexpression of HER2 are currently treated with the targeting agent trastuzumab, the only anti-HER2 treatment of metastatic breast cancer approved by the FDA to date. Treatment with trastuzumab alone is not a form of radiotherapy since no radionuclide is used in the treatment process. Trastuzumab can however, be used in combination with other kinds of cancer therapy such as chemotherapy and external beam radiotherapy. The trastuzumab molecule weighs approximately 185 kDa and binds with high affinity and specificity to the HER2-receptor [19]. The introduction of trastuzumab has introduced a shift in breast cancer treatment. Indeed, trial studies have shown that, regardless of tumor size, nodal status or time of administration, the addition of trastuzumab improves the survival rate by 30 % and reduces recurrence by 50 % [20]. Although not all mechanisms are fully understood, the effect of trastuzumab includes apoptosis through reduction of receptor signaling and inhibition of angiogenesis through the removal of HER2 from the cell surface [21].

Affibody molecules

Affibody molecules are engineered affinity proteins designed to target and bind specifically to a number of different target proteins. They are produced by phage display (Affibody AB, Stockholm). The Affibody molecule used in this study is a synthetically produced HER2-binding variant denoted as $Z_{HER2:342}$ (PEP05352), and binds to the HER2-receptor with high affinity [22]. The chemical structure of the Affibody that was used allowed for direct labeling with ^{99m}Tc and thus no conjugation of any chelate was necessary.

---

[1] Receptor tyrosine kinases are high-affinity cell surface receptors involved in cell signaling
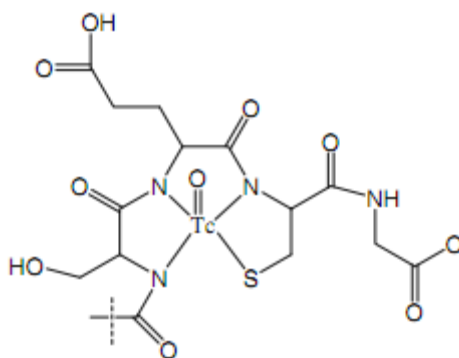
Figure 2.1 *Chelator structure of the Affibody molecule. The border to the Affibody molecule center is indicated by the dashed line. Image taken with permission from Tran et al. [23].*

Because of its relatively small size, maximum tumor uptake should occur faster than that of trastuzumab. In a preclinical study by Tran et al. tumors in nude NMRI mice were clearly visualized after 4 h.p.i [23]. This makes [99m]Tc ($T_{1/2}$ ~ 6 h) the most suitable radiotracer for Affibody, while the larger molecule trastuzumab will be labeled with [111]In ($T_{1/2}$ ~ 2,8 d).

2.4 Radionuclides

In this study, two radionuclides were used as for radiolabeling of traztuzumab and Affibody molecules: [99m]Tc and [111]In. Both radionuclides are chemically stable as ^{99m}Tc-pertechnetate ([99m]TcO$_4$-) and ^{111}In-chloride ([111]InCl$_3$) (liquid form). Throughout the experiment, these two compounds were used exclusively with a few exceptions for ^{111}In-chloride, which at some points were substituted with ^{111}In-octreotate. This substitution was only used for calibration of instruments and was not considered to have any impacts on the calibrations.

[99m]Tc is the most common radionuclide used in clinical nuclear medicine procedures, largely due to its favorable emissions, low cost, relatively short half-life and availability. It is well suited for small animal SPECT as well with its 140,5 keV photon that easily penetrates the body of a mouse with little attenuation (~10 %). [99m]Tc has a half-life of 6 hours and is easily produced in and extracted from [99]Mo/^{99m}Tc-generators.

[111]In emits two gamma photons at 171,3 and 245,4 keV and has a half-life of 67,3 hours. This makes ^{111}In easy to distinguish from ^{99m}Tc in a gamma detector, and makes both radionuclides a fitting pair for dual-radionuclide measurements. In the case of the scintillation counter the summation peak of ^{111}In is used, rather than measuring the two photons separately, making the photo peak even more distinguishable from [99m]Tc. Their difference in half-life is exploited at several occasions in this work, the most notable being the choice of which molecule to fit with which radionuclide. Both radionuclides emit conversion and Auger electrons as well, making autoradiography possible. For decay characteristics of both radionuclides, see table 2.1.

Table 2.1 *Decay characteristics of ^{99m}Tc and ^{111}In. Data is taken from the MIRD-database.*

^{99m}Tc			^{111}In		
Emission type	Energy [keV]	Yield [Bq-s]$^{-1}$	Emission type	Energy [keV]	Yield [Bq-s]$^{-1}$
γ1	140,5	0,89	γ2	171,3	0,91
Kα1 X-ray	18,4	0,04	γ3	245,4	0,94
Kα2 X-ray	18,3	0,02	Kα1 X-ray	23,2	0,44
Kβ X-ray	20,6	0,01	Kα1 X-ray	23,0	0,24
Auger-K	15,5	0,02	Kβ X-ray	26,1	0,15
Ce-K γ 2	119	0,08	Auger-K	19,3	0,15
			Ce-K γ 2	144,6	0,08

2.5 Measurement protocols

The primary goal of this work is to evaluate each instruments capability to correctly quantify two radionuclides simultaneously. The principal challenge lies in the fact that all instruments, except for the one used for digital autoradiography, has built-in functions for these types of measurements. Much modern equipment corrects automatically for factors such as decay, background and crosstalk. Although practical, this limits the possibility to use machines for specially tailored situations and also diminishes flexibility. It becomes especially challenging when the algorithms under which these corrections work are unknown to the user. One can observe results from phantom measurements and correct for systematic errors, but theorizing over the cause of these errors is significantly harder without knowing how the system works.

Crosstalk refers to the contribution from one energy window to another. This means that if two radionuclides are measured simultaneously, they can contribute to each other's energy windows e.g. through scattering processes. In particular, radionuclides with higher energy emissions could contribute through down-spill to regions of lower energy.

In order to evaluate the dual-radionuclide protocols[2], it is assumed that the single-radionuclide measurements represent a correct value of the activity. The principal idea is that if the quantitative results of the dual-radionuclide measurements match those of the single-radionuclide measurements, the automatic crosstalk correction functions properly and no further corrections have to be done. Should the results display a systematic error, then this should be possible to correct for.

When performing biodistribution studies, i.e. determining uptake in different tissues at several points in time, the concentrations of two different molecules will, because of different traits such as size and molecular structure, vary in different tissues. For example, previous studies show an early, high uptake of Affibody in the kidneys of mice, whereas the trastuzumab uptake in the same organ is relatively low. In contrast, trastuzumab uptake in the liver has shown to be quite high, while Affibody uptake is very low [23, 24]. The relationship between the two measurement protocols should be examined as a function of different concentrations of the two radionuclides used in the experiment. This was the principal idea – one set of phantoms containing different amounts of ^{99m}Tc and another

---

[2] Measuring two radionuclides at the same time with one or more energy windows using the instruments built-in functions for crosstalk correction will be referred to as *dual-radionuclide measurement*. The settings that are used will be referred to as the *dual-radionuclide protocol*. Correspondingly, measuring only one radionuclide with one or more energy windows, not using these functions will be referred to as single-radionuclide measurement or protocol respectively.

[111]In are measured separately using single-radionuclide protocols and compared to a set of phantoms containing the same amount but this time with both radionuclides in the same phantoms. Should there be any deviations between the single and dual-radionuclide protocol it should then be possible to correct for this based on parameters such as different concentrations and dead-time.

This approach will be used for all three instruments. The difference is that for the small animal SPECT and the scintillation counter the dual-radionuclide protocols that are being evaluated already exist in the machine software. In the case of digital autoradiography, in-house, purpose written software that is used to separate the radionuclides will be evaluated.

2.6 Dead time

Dead time specifically refers to the minimum amount of time that must separate two events in order for them to be registered as two separate pulses. Should two events occur within this time window, they will be recorded as one pulse by the detector system and thus information is lost. In a *non-paralyzable* system this dead time is fixed, regardless of true count rate. In contrast, a *paralyzable* system like the scintillation counter will, given a high enough true count rate, lose more counts due to an extended dead time. In the paralyzable model, the recorded count rate m is related to the true interaction rate n and the dead time τ by the following expression:

$$m = ne^{-n\tau}$$

It is clear that n cannot be solved for analytically. The scintillation counter used in this work could best be described by the paralyzable model. Because of this, experiments designed to correct for dead time-related errors were performed but was, due to lack of time, never implemented. Instead only data from activity levels where the effects of dead time could be ignored was used.

3 Materials and methods

3.1 Radiolabelling of traztuzumab and Affibody

The following sections describe how trastuzumab and Affibody were labeled with their respective radionuclides. Trastuzumab, being labeled with ^{111}In, could be prepared several days in advance whereas Affibody was labeled on the same day as the experiment. Labeling efficiency and radiochemical purity were estimated through a series of quality control procedures.

3.1.1 Conjugation and radiolabelling of trastuzumab

In order to label trastuzumab with ^{111}In it must first be conjugated with a chelator. The chelating agent used in this experiment was CHX-A''-DTPA[3] (Macrocyclics, USA). A sodium borate buffer was used to serve as a stable environment for the antibody and the chelator. The buffer was prepared with pH ~9,2 and a concentration of 0,07 M. The trastuzumab was originally delivered in a NaCl-buffer and thus the solution first needed to undergo buffer exchange. This was done using a NAP-5 column (GE Healthcare). Consisting of a gel-matrix with pores of different sizes, the NAP-5 column can be used to separate molecules of

---

[3] DTPA - diethylene triamine pentaacetic acid, whose conjugate base easily binds to metal ions and is often used as a chelating agent in medicine

different sizes; larger molecules will not be trapped in the matrix and will consequently pass the column faster than smaller ones. Firstly the NAP-5 column was equilibrated with 25 mL of the buffer solution. Secondly 0,5 mL of trastuzumab (21mg/mL in PBS) was added to the equilibrated column. The NaCl will pass the column and the trastuzumab molecules will be left in the column. The column is then eluted with 1 mL of the sodium borate buffer. The end result is trastuzumab in a sodium borate buffer. The pH-value of the solution was measured and estimated to be between 9-9,5.

The chelating substance was prepared separately. A total of 0,4 mg CHX-A''-DTPA was added to 10 microliter of sodium borate buffer. For the conjugation, 1 μl CHX-A''-DTPA was added to 200 μl of trastuzumab. This saturates the solution with CHX-A''-DTPA. The solution was then incubated for 4 h at 40°C. After conjugation, the solution was separated on a NAP-5 column and eluted with 0.2 M sodium actetate, pH 5.5. The conjugate was aliquoted in small portions of 100 μl and was stored in -20°C.

For radiolabelling, 50 μg of DTPA-trastuzumab was mixed with ^{111}In-chloride (~100 MBq) and incubated for 60 min in room temperature. After reaction, radioconjugate was purified on a NAP-5 column as above and eluted in PBS.

3.1.2 Radiolabelling of Affibody

For the labeling process, 24 μg of Affibody solution (1 mg mL^{-1} MQ-water[4]) was used with 20 μg 0,15 M NaOH at pH ~11 and 10 μg of SnCl$_2$ ·2 H$_2$O (1mg/mL HCl). Free^{99m}Tc-pertechnate (~300 Mbq) was added to the mixture which was then incubated for a period of 60 minutes.

During incubation, a NAP-5 column was equilibrated with 25 mL of phosphate buffered saline (PBS[5]). In this process, the NAP-5 column will be used to separate successfully labeled molecules from impurities; labeled molecules will be larger than non-labeled ones and thus pass through column quicker. The now labeled Affibody solution is placed in the column, along with 0,5 mL of PBS solution. The column was then placed over a sample tube and eluted with 1 mL of PBS. This should now contain only the successfully labeled molecules. The column was placed over another sample tube and PBS buffer is applied one more time. This column should now only contain free ^{99m}Tc-pertechnetate.

3.1.3 Quality control

Quality control was carried out using instant thin layer chromatography (ITLC) strips. An ITLC method consists of a *stationary phase* and a *mobile phase*. The stationary phase is the actual strip; fiberglass sheets impregnated with silica gel. For the mobile phase a PBS-buffer solution was used for ^{99m}Tc-Affibody and 0.2 M citric acid was used for ^{111}In-trastuzumab. A small drop (~1 μL) of the labeled compound is placed on the strip (see figure 3.1). The mobile phase is then applied at the bottom the strip and will then slowly migrate upwards. The successfully labeled molecules will remain stationary at the bottom of the strip, whilst any non-labeled molecules will follow the eluent front.

---

[4] MQ-water or Milli-Q water, the trademark name for a de-ionized ultra-pure water product
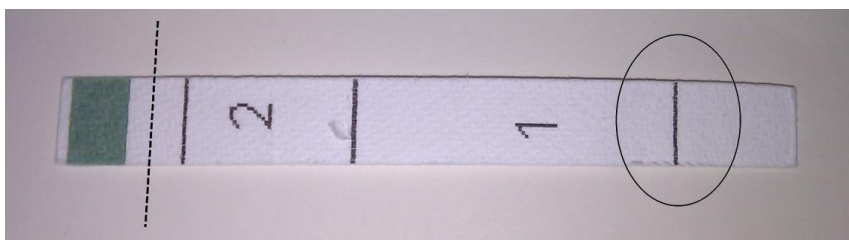[5] PBS - Phosphate Buffered Saline, a buffer solution commonly used in biological research

Figure 3.1 *A picture of an ITLC-strip. The solution is placed on the line within the circle. The non-labeled molecules will then follow the eluent front towards the dotted line, whilst the successfully labeled molecules remain.*

This test was performed for both the ^{99m}Tc-labeled Affibody molecules and ^{111}In-labeled trastuzumab. The strips are evaluated in the OptiQuant image analysis software using the Cyclone Storage Phosphor System (Perkin Elmer , Waltham, MA, USA). ITLC-strips are placed on a phosphor imager plate. The now excited atoms on the plate remain in their excited state until the phosphor imager scans the plate with a laser. The phosphor imager produces a 2-dimensional image of the activity distribution of the ITLC-strips that can be quantitatively analyzed in the OptiQuant software. The radiochemical purity of all labeled compounds exceeded 98 %.

3.2 Development and evaluation of dual radionuclide protocols

In this study three imaging modalities and detectors were used. All instruments except the Biomolex 700 Imager used for digital autoradiography have the option of dual-radionuclide measurements included in the system software.

3.2.1 Scintillation counter

The Wallac WIZARD 1480 3'' scintillation-counter (Wallac, Turku, Finland) uses a 3'' NaI(Tl)-crystal to detect photons in the range 15 – 2000 keV. It is primarily designed to count high photon energy emitting samples with relatively low activity and can, if calibrated correctly, estimate the activity of those samples with high accuracy. In preclinical research it is often used for biodistribution studies. By determining the activity in an organ – or part of an organ – it is possible to estimate the uptake in that organ at a specific point in time. The scintillation counter utilizes a barcode system when measuring samples; racks are fitted with barcode-tags which, upon entering the detector, will initiate a certain protocol with predefined measuring parameters such as measuring time and energy window settings. These parameters are defined by the user and can easily be changed at any time. All calibrations of the system were based on two calibrated scintillation counters at the radionuclide center (RNC) used in clinical practice. An LKB Wallac laboratory scintillation counter (1282 Compugamma, LKB Wallac, Turku, Finland), and a WIZARD 1480 were used for ^{99m}Tc and ^{111}In respectively. The window settings that were used in the experiments were the same as the scintillation counters at the RNC. Energy window settings for both radionuclides are displayed in table 3.1.

Table 3.1 *Energy window settings for the scintillation counter. These settings were used for all scintillation counter measurements*

	Energy window 1
[99m]Tc	140,5 ±13%
[111]In	171,3 ±13%

The system allows for simultaneous measurement of two radionuclides. This is referred to as "dual-label counting" in the scintillation counter software and manual. The creation of a dual-label protocol is performed simply by combining two single-label protocols.

Volume calibration

Before the scintillation counter can be used to quantify activity, it needs to be calibrated. This was done partly by normalizing the detector for a certain radionuclide; another automatic procedure, and calibrating for volume sensitivity. All phantom measurements were performed using scintillation-counter test-tubes. The more liquid these tubes contain, the more photons will attenuate and scatter and will be missed by the detector, resulting in a loss of counts and, consequently, an incorrect quantification. Apart from information about the time of measurement, rack position etc. the output from the scintillation counter is total number of counts, counts per minute and dead-time factor.

The dead time factor is used by the scintillation counter to correct for higher activities when the flux of incident photons is too high and represents the difference between actual count rate and observed count rate. The output used for determining the activity is counts per minute, which is obtained by dividing the total number of counts registered with the dead-time correction factor. However if one would measure the same activity over and over again and add water into the test-tube between each instrument, one would observe a drop in the counts per minute output because of photon attenuation and scattering. Consequently, the scintillation counter needs to be calibrated for volume sensitivity. Because of the different emission spectra, this needs to be done for each radionuclide. Two spectrums of ^{99m}Tc and ^{111}In obtained from the scintillation counter can be seen in figure 3.2 and 3.3.
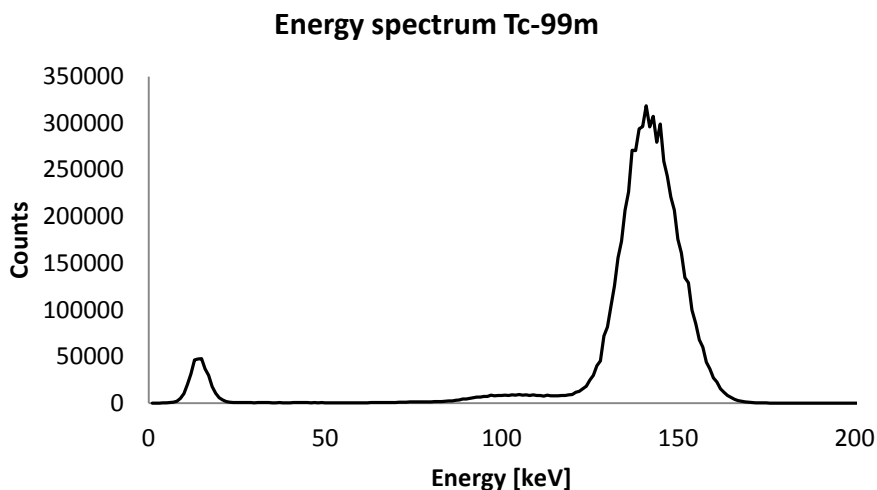

Figure 3.2 *Energy spectrum of ^{99m}Tc obtained with the Wallac scintillation counter. The activity in the sample was about 10 kBq with a measurement time of ten minutes.*
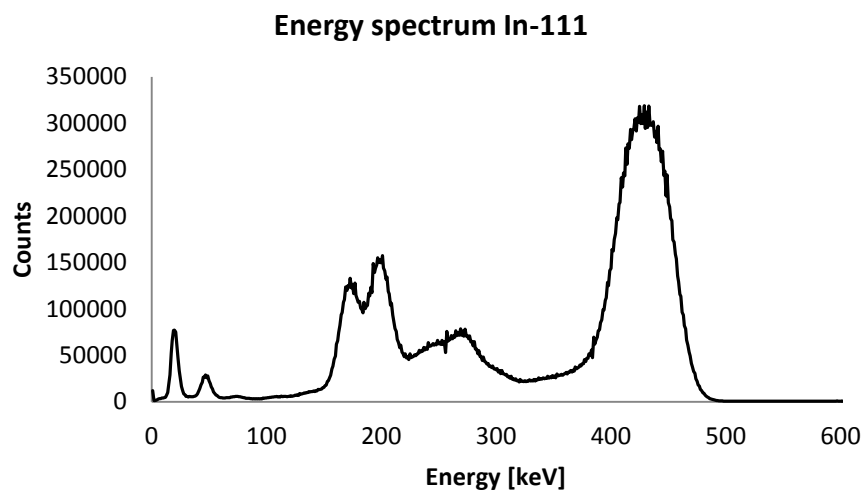
Energy spectrum In-111

Counts (y-axis): 0, 50000, 100000, 150000, 200000, 250000, 300000, 350000

Energy [keV] (x-axis): 0, 100, 200, 300, 400, 500, 600

Figure 3.3 *Energy spectrum of the radionuclide* ^{111}*In obtained with the Wallac scintillation counter.*
The summation peak is clearly visible at around 420 keV.

In order to create a calibration curve for the scintillation counter a batch solution of about 12 kBq of ^{99m}Tc-pertechnate was distributed between three scintillation counter test tubes and measured for 3 minutes each, for a total number of 40 times, each measurement generating >100 000 counts. Energy windows were set to 121-159 keV for ^{99m}Tc and 380-495 keV for ^{111}In. These energy settings were used for all phantom measurements as well as for the pilot animal study. Between each measurement, water was added with an air-displacement pipette. Activity concentration of the initial batch was determined by measuring the activity with a clinical scintillation counter and the amount of ^{99m}Tc-pertechnate in grams with a high-sensitive scale (Mettler-Toledo, Columbus, US). Test tubes were weighed between each measurement to determine the volume for each data point. Values were the plotted as cpm/Bq as function of the volume V. The results were later fitted with a polynomial, whose equation could be used to obtain a correction factor for a certain volume. The same procedure, but with 9 measurements instead of 40, was then repeated for ^{111}In .
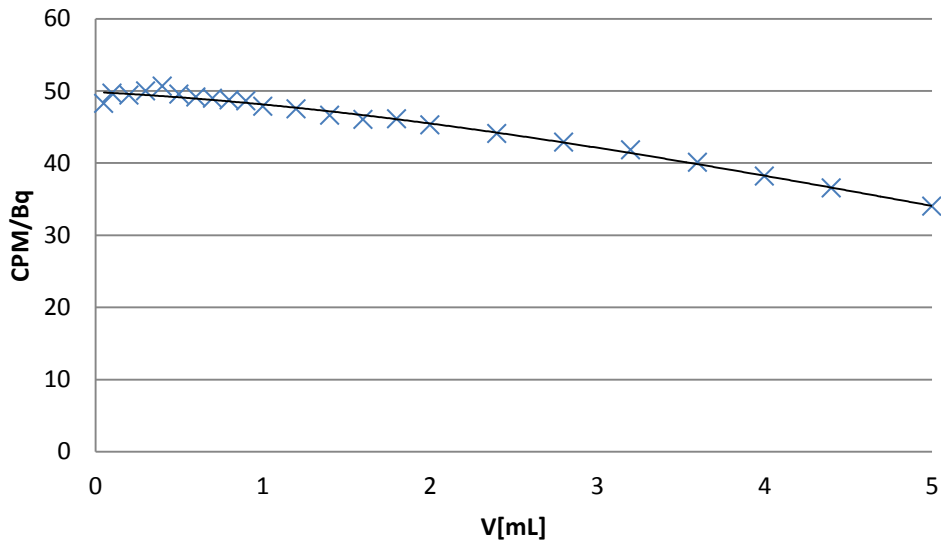
Volume correction Tc-99

Figure 3.4 Calibration curve for ^{99m}Tc.
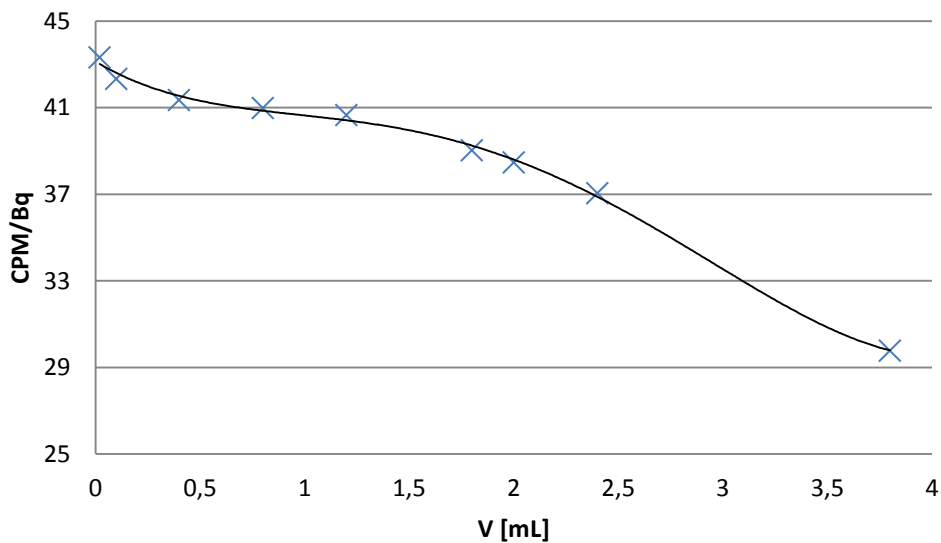
Volume correction In-111

Figure 3.5 Calibration curve for ^{111}In.

The activity of a sample can now be determined by dividing the counts per minute output from the scintillation counter with the calibration factor.

Phantom measurements

All test tubes in the experiment were weighed prior to and after dispensation of any activity. Firstly, the single-radionuclide protocol (for ^{99m}Tc) was used to measure the activity of 9 test-tubes, all containing different amounts of ^{99m}Tc-pertechnetate, ranging from 0,2-3,8 kBq. All test-tubes were measured for 180 s. Different amounts of ^{111}In-chloride were then added so that the total activity of both radionuclides combined in every tube was 4 kBq. These tubes were then measured with the dual-label protocol for 180 s each. Due to

the relatively short half-life of ^{99m}Tc (6 h) compared to that of ^{111}In (67,7 h), the most practical approach was to wait for ^{99m}Tc to decay sufficiently and measure the remaining ^{111}In. The remaining ^{111}In was measured for 180 s using the single-label protocol for that radionuclide.

The data was analyzed by comparing the ratios of measured activity between the two single-radionuclide protocols and the dual-radionuclide protocol.

3.2.2 Digital Autoradiography

Digital autoradiography can be used to study the spatial distribution of molecules in tissue-samples on a micrometer scale. The instrument that was used for autoradiography in this study is the Biomolex 700 Imager (Biomolex AS, Norway) and it has a spatial resolution of ≥50 µm and measures charged particles in the >15 keV range. It utilizes an automatic sample handling system capable of measuring 12 samples consecutively where microscope slides are used to contain samples (see fig. 3.5). The detector system is comprised of a solid state, double sided silicon strip detector.

Photons, having a longer mean free path than charged particles in general, will as a rule escape the detector, avoiding detection. However, low-energy photons might not and can degrade spatial resolution. These photons can travel quite far from the decay site before they deposit their energy, blurring the picture somewhat, as illustrated in figure 3.7. This is especially a problem for ^{111}In, which emits two x-ray photons at 23,17 and 22,98 keV. It is possible to correct for this by simply removing events below a certain threshold energy. This leads to a loss in statistics but can improve the image quality (figure 3.2).
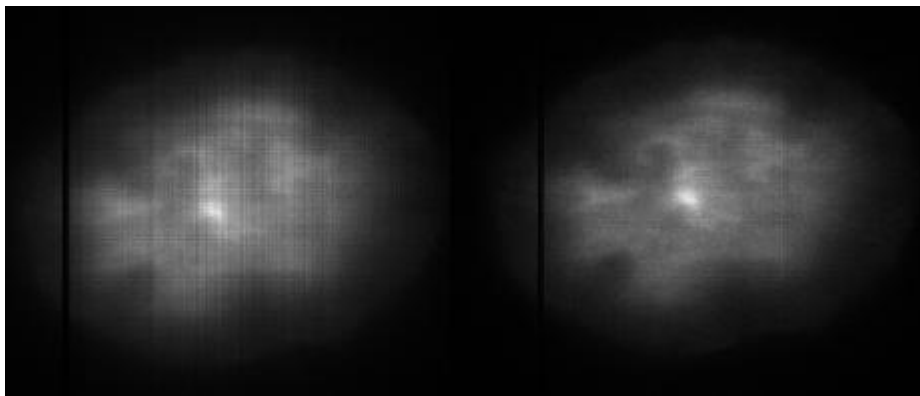

Figure 3.6 *Example of the effects of removing the low-energy photon peak from the ^{111}In-spectra. By removing the low energy photons, a sharper picture can be achieved (right).*

The Biomolex 700 Imager has both spatial, temporal and energy resolution. Data is stored in list-mode and can be extracted and analyzed after measurement. As mentioned earlier, the Biomolex 700 does not have a built in function for dual-radionuclide measurement. The extracted data contains information from both radionuclides and must be separated. This was done by using in-house software written in IDL 6.4[6] (ITT Visual Information Solutions, NY, USA).

---

[6] IDL – Interactive Data Language. A programming language commonly used in astronomy and medical imaging.

Figur 3.7 *The Biomolex 700 Imager.*

Efficiency

Efficiency was determined for both radionuclides. Two samples, small paper strips initially soaked in ^{99m}Tc-pertechnate and ^{111}In-chloride respectively and then air-dried, were measured long enough to display characteristic decay curves (4 h for ^{99m}Tc and 31 h for ^{111}In). Decay curves are plotted in IDL as registered counts per time interval. To determine the original count rate, the resulting curves were fitted against curves representing the theoretical decay of each radionuclide in IDL. This curve fit is used to determine the original count rate. The remaining activity in each sample was determined by dissolving them in hydrochloric acid and measuring them in the scintillation counter. This way the original activity could be determined and efficiency for each radionuclide calculated. The results are displayed in table 2.1.

Table 3.2 *Biomolex efficiency results.*

	Efficiency [cps/Bq]
^{99m}Tc	0,052
^{111}In	0,19

Phantom measurements

Small drops of activity were placed on small paper strips using air-displacement pipettes. In order to avoid problems with dead-time during measurements count-rates were kept under 400 cps. Initially, a total of 8 paper strips placed in microscope slides were measured individually for 20 minutes, each strip with different amounts of ^{99m}Tc-pertechnetate, yielding as much as 400 cps for the strip with the largest activity. For the dual-radionuclide measurements, ^{111}In-chloride was added on each strip so that the total cps for each would be about 400 cps. These were measured for 40 minutes each. After the ^{99m}Tc had decayed sufficiently, the individual strips were yet again measured for another 20 minutes.

Separation of radionuclides

As previously mentioned, the Biomolex 700 Imager has both spatial, temporal and energy resolution. In order to successfully separate the radionuclides, the latter two were used. For each count the instrument detects, information about energy and time of detection is stored. In order to use this information to tell the radionuclides apart, their respective spectra were studied and compared. Three energy-regions (or bins) were chosen so that

the contribution from each radionuclide would be different enough to tell them apart while keeping the counts in each region somewhat similar. To achieve this, both spectra were normalized and the areas in each region compared to one another. The energy windows can be seen in figure 3.6. Each radionuclide will have a characteristic contribution in each window that yields a correction factor that the program uses to determine the likely origin of each count.
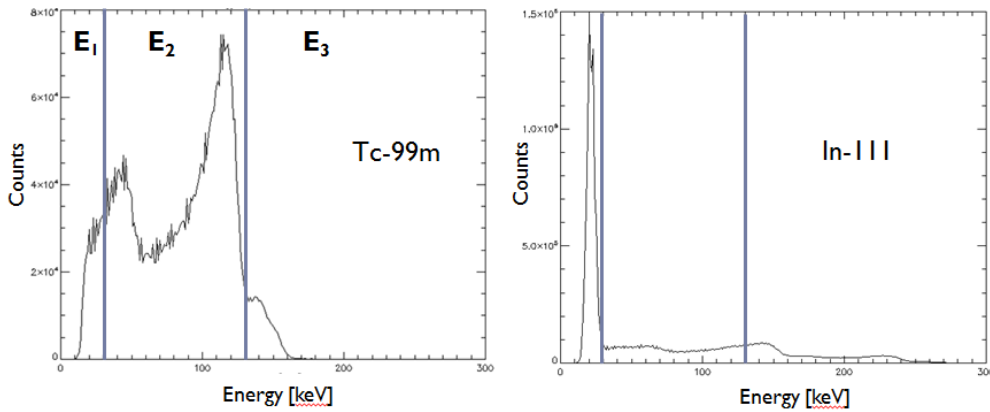

Figure 3.8 *Energy spectra from both ^{99m}Tc and ^{111}In. Both spectra were plotted using IDL.*

The program sorts each count from the single-radionuclide measurements into the predefined time and energy bins. The arrays created in this step provide the program with templates for both radionuclides. These templates ends up populating matrices "radionuclide 1" and "radionuclide 2", whilst the dual-radionuclide measurement data will end up in the "data" matrix.

$$\begin{Bmatrix} x_{11} & x_{12} & x_{12} \\ x_{21} & x_{22} & x_{23} \end{Bmatrix}_{Data} = R_1 \begin{Bmatrix} y_{11} & y_{12} & y_{13} \\ y_{21} & y_{22} & y_{23} \end{Bmatrix}_{isotope\ 1} + R_2 \begin{Bmatrix} z_{11} & z_{12} & z_{13} \\ z_{21} & z_{22} & z_{23} \end{Bmatrix}_{isotope\ 2}$$

In the separation process the program will, one pixel at a time, iterate all possible combinations of single radionuclide templates and use the method of least squares to find the two coefficients R_1 and R_2.

3.2.3 Small animal SPECT/CT

In this study the NanoSPECT/CT imaging system was used (Bioscan, Washington, DC, USA). The system utilizes four NaI detectors with multi-pinhole collimators (NSP-106 mouse collimator) for high spatial resolution. Each pinhole is 1 mm in diameter and each collimator has 9 pinholes. The system measures photons in the 20-200 keV range and allows for simultaneous data acquisition of more than one radionuclide. The cross-talk correction is performed automatically by the system with the only prerequisite being calibration of the camera for both radionuclides. The exact procedures within the system of this feature are unknown and so this process was therefore evaluated in the same manner as with the scintillation counter.

The NanoSPECT/CT was calibrated for both ^{99m}Tc and ^{111}In using a well-type ion-chamber (Capintec, Ramsey, NJ, USA) as a reference. A dual-radionuclide protocol was created using the SPECT/CT-software. Energy windows were centered around the 140,5 keV photopeak for ^{99m}Tc and the two photopeaks at 171,3 and 245,4 photopeaks for ^{111}In. Energy window settings for both radionuclides are displayed in table 3.2.

Table 3.3 *Dual-radionuclide protocol energy window settings for ^{99m}Tc and ^{111}In in keV.*

	Energy window 1	Energy window 2
^{99m}Tc	140,5 ±10%	
^{111}In	171,3 ±10%	245,4 ±10%

Phantom measurements

All phantom measurements were performed using scintillator-counter test tubes that were placed in a cylindrical water phantom (to emulate the conditions of an animal study using mice) in the same set-up that were used in the animal pilot study.

Figure 3.9 *Phantom measurement set-up.*

The dual-radionuclide protocol was evaluated by comparing its ability to correctly quantify a known amount of activity to the single radionuclide protocols for each radionuclide.

A total of six scintillation-counter test-tubes were filled with different amounts of activity of ^{99m}Tc-pertechnetate, ranging from 2 to 10 MBq, and imaged with the single-radionuclide, helical scan protocol for 40 minutes each, generating > 100 000 counts in each detector. CT-scans were also taken for all tubes. The same test-tubes were then filled with different amounts of ^{111}In-chloride so that all test-tubes contained about 10 MBq each. These were imaged under the same conditions with the dual-radionuclide protocol. After the ^{99m}Tc-radionuclide had decayed to sufficiently low levels, the test-tubes were measured yet again using the single-radionuclide settings.

Images were reconstructed using a maximum-likelihood expectation maximization (MLEM) algorithm in the HiSPECT-software (Bioscan, Washington, DC, USA). Images were evaluated in the Bioscan InVivoScope^{TM}: Molecular Imaging Suite (Bioscan, Washington, DC, USA).

3.3   Animal pilot study

All animal studies were approved by the regional committee on animal experiments and performed in accordance with Swedish law. Ten normal non-tumor bearing NMRI mice (male and female) were divided into three different groups; two of the groups were injected with one of the two selected molecules, and the third group was injected with both. Injection procedures, radioactive compound and the total amount of activity for each group are illustrated in table 3.1.

Table 3.4 *Injected molecules, number of animals, activity and injection type for all groups.*

Group	Number of mice	Radionuclide	Activity [MBq]	Injection type
1	3	^{99m}Tc-Affibody	40	Intraperitonial
2	3	^{111}In-trastuzumab	10	Intravenous
3	4	^{99m}Tc-Affibody+^{111}In-trastuzumab	30+10	Intraperitonial

Figure 3.10 *An NMRI mouse prior to imaging. The mouse is provided with a sufficient flow of isoflourane to keep it anaesthetized and warm air to keep the body temperature stabilized.*

Prior to imaging, mice were placed in a specially constructed hibernation chamber and anaesthetized using 1-3% isoflourane. Anaesthetized mice were then transferred to the mouse bed where they remained anaesthetized for the duration of the imaging. A built in heating-system kept the body-temperature stabilized. All animals were imaged for about 40 minutes (excluding x-ray scouts and CT-images)[7] using a helical scanning protocol. Images were reconstructed using the HiSPECT-software using an MLEM-algorithm.

Mice were sacrificed using a CO_2-mixture and dissected. The organs that were extracted were either kept in scintillation counter test-tubes for later measurements in the scintillation counter or frozen in embedding media (O.C.T., Tissue Tek, PA, USA) for later sectioning with the cryostat. Organs were sectioned in 10, 20 and 30 µm thickness and imaged with the Biomolex 700 digital autoradiography system.

---

[7] X-ray scouts are planar x-ray images used for orientation

4   Results

4.1   Phantom measurements

The results from all phantom measurements are displayed in the graphs below. Figures 4.1, and 4.2 display the relationship between the single and dual-radionuclide protocols. Each data point represents the relationship between the activity as determined by the single-protocol and dual-protocol for a certain mixture of the two radionuclides. The difference between the protocols is plotted as a function of the amount of ^{99m}Tc in the mixture.
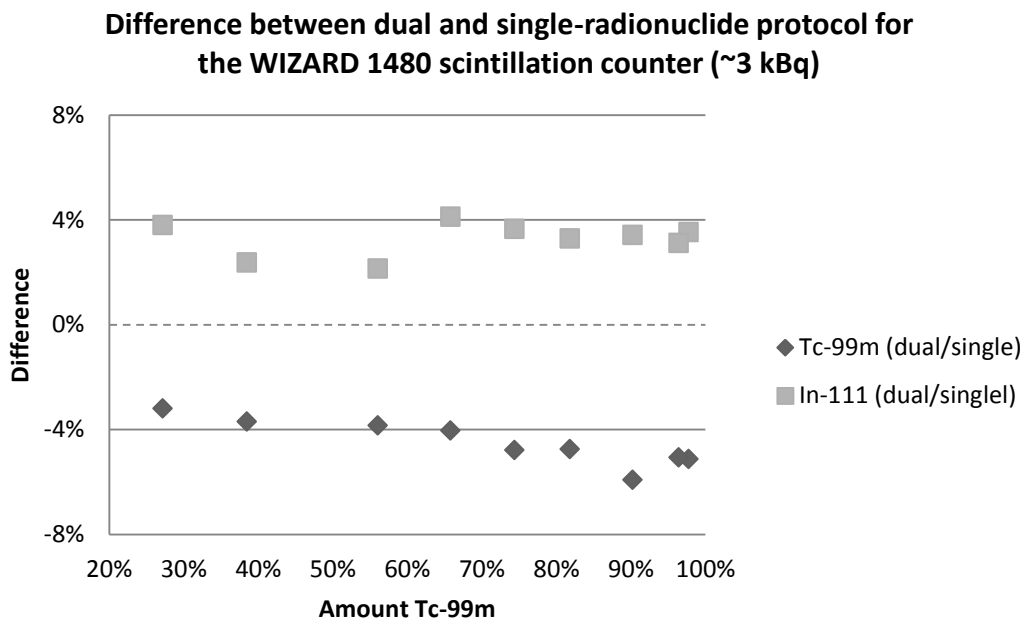

Difference between dual and single-radionuclide protocol for the WIZARD 1480 scintillation counter (~3 kBq)

Figure 4.1 *Results from scintillation counter measurements. The total activity in each sample tube was 4 kBq. Average dead time-factor for all data points was 1.03.*

Figure 4.1 one shows that dual-radionuclide protocol overestimates ^{111}In with a mean value of 3,2 % while it underestimates ^{99m}Tc with a mean value of 4,7 %. There are no visible trends for either of the protocols. As samples with higher activities are examined, the results are different. In a different experiment performed later, a higher activity was used as well as more data points. This can be seen in figure 4.2. Here, ^{111}In is underestimated for all concentrations but with a clear trend as the concentrations change. The dual-radionuclide protocol initally overestimates ^{99m}Tc, but as the concentration of ^{99m}Tc increases and ^{111}In decreases, so does the relationship between the protocols.

**Difference bewteen dual and single-radionuclide protocols
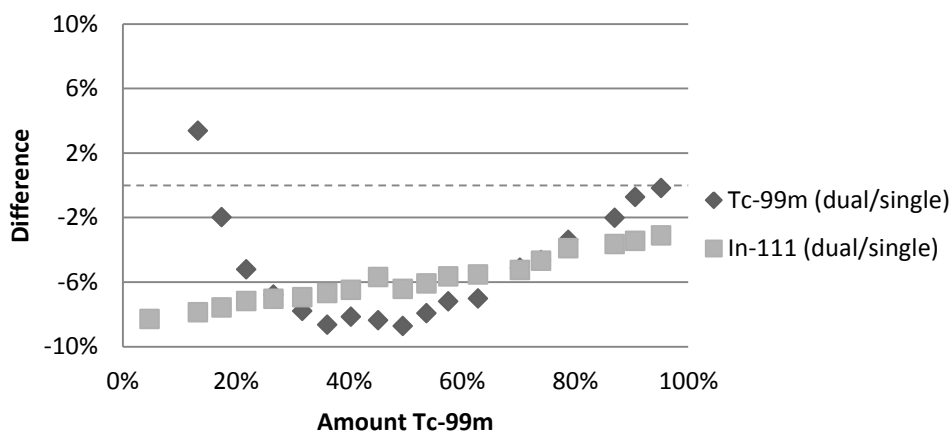for the WIZARD 1480 scintillation counter (~25 kBq)**

Figure 4.2 *Results from gamma counter measurements. The total activity in each test tube was about
25 kBq. The average dead time-factor for each measurement was 1.28.*

The Biomolex 700 imager initially overestimates ^{99m}Tc. As the amount of ^{99m}Tc
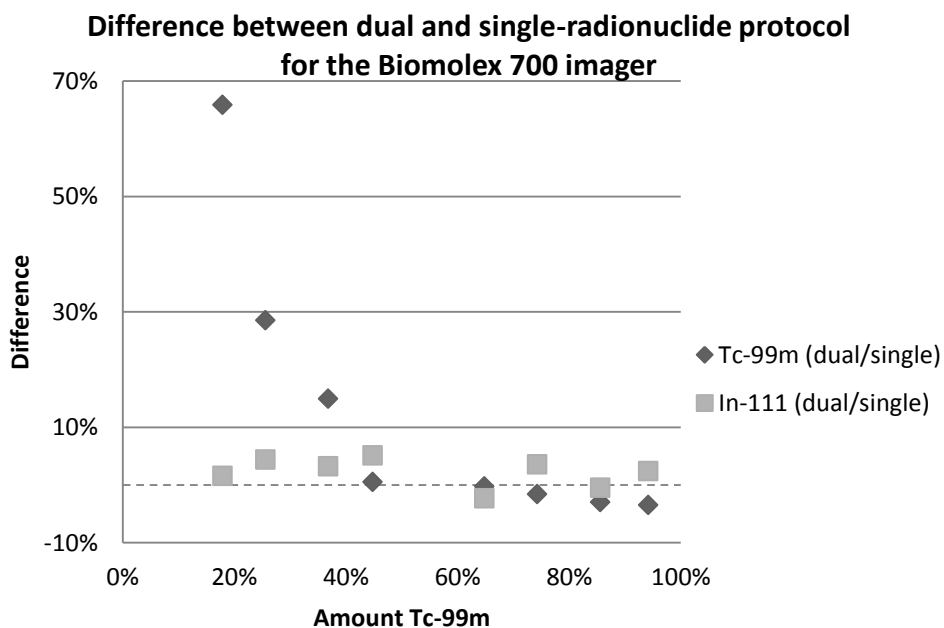increases, the curve quickly decends.

**Difference between dual and single-radionuclide protocol
for the Biomolex 700 imager**

Figure 4.3 *Results from the Biomolex instrument.*

The NanoSPECT/CT system overestimates both radionuclides except for higher
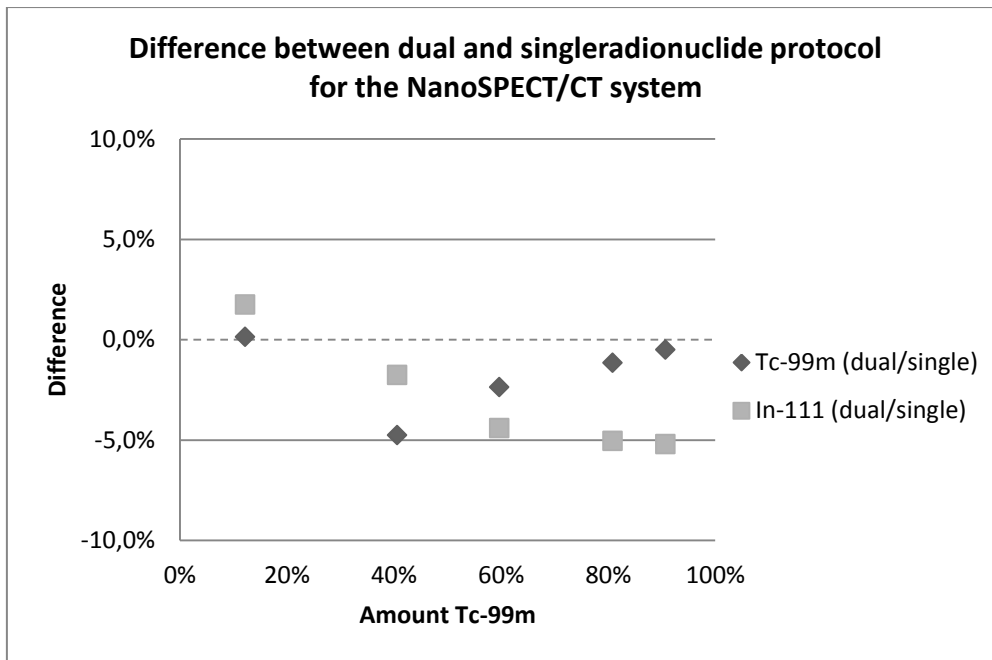concentrations of ^{99m}Tc.

Figure 4.4 *Results from SPECT measurements. The total activity in each test tube was about 10 MBq.*

4.2 Animal pilot study

Several images were acquired during the animal pilot study. Below are a few selected examples showing uptake of both Affibody and trastuzumab. As expected, there was a high uptake of trastuzumab in the liver (figure 4.5) whilst most of the Affibody uptake occurred in the kidneys. Due to the kinetic properties of Affibody, there was also a high concentration in the bladder. Uptake of ^{99m}Tc-Affibody was also observed in the mediastinal lymph nodes (figure 4.5 and 4.6). A higher uptake in the cortex was also observed, shown in figure 4.8.
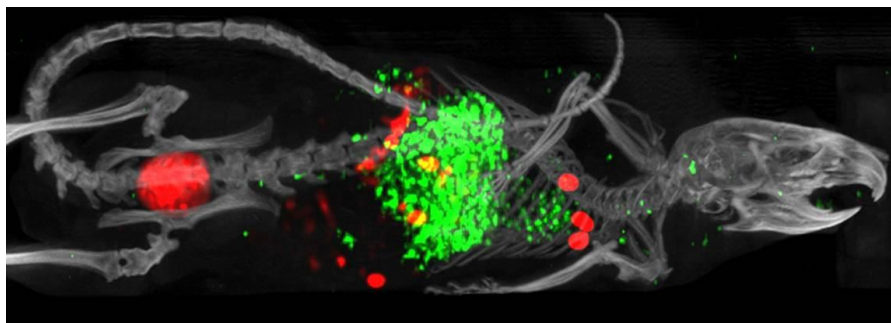

Figure 4.5 ^{111}*In-trastuzumab (green) and* ^{99m}*Tc-Affibody (red) uptake in mice 6 h.p.i. High concentration of trastuzumab can be seen in the liver. Affibody uptake is visible in the bladder and the mediastinal lymph nodes.*
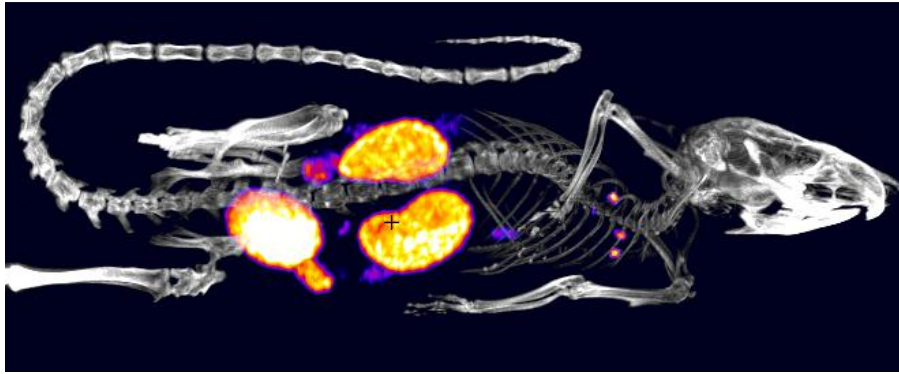
Figure 4.6 ^{99m}*Tc-Affibody uptake in NMRI mouse 6 h.p.i. Kidneys and bladder are clearly visible. Uptake in the mediastinal lymph nodes can also be observed.*

Figure 4.7 shows trastuzumab uptake in a mouse taken with a single-radionuclide protocol. Most of the uptake is observed in the liver. There is also a higher concentration at the site of injection in the tail.
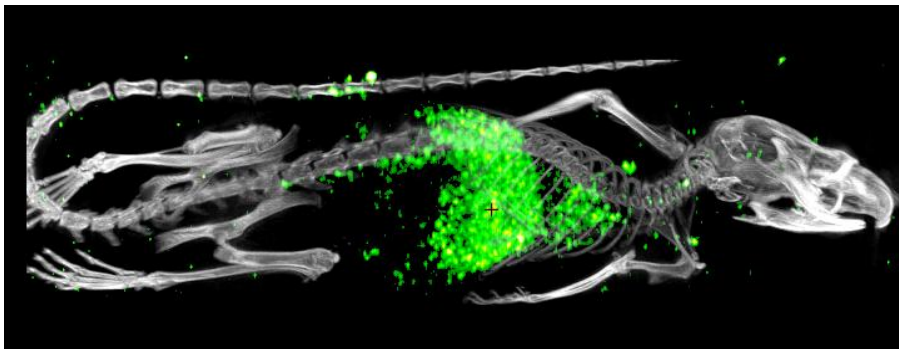

Figure 4.7. ^{111}*In-trastuzumab uptake in NMRI mouse 16 h.p.i. High concentration in the liver. A few hotspots can be seen at the point of injection in the tail.*
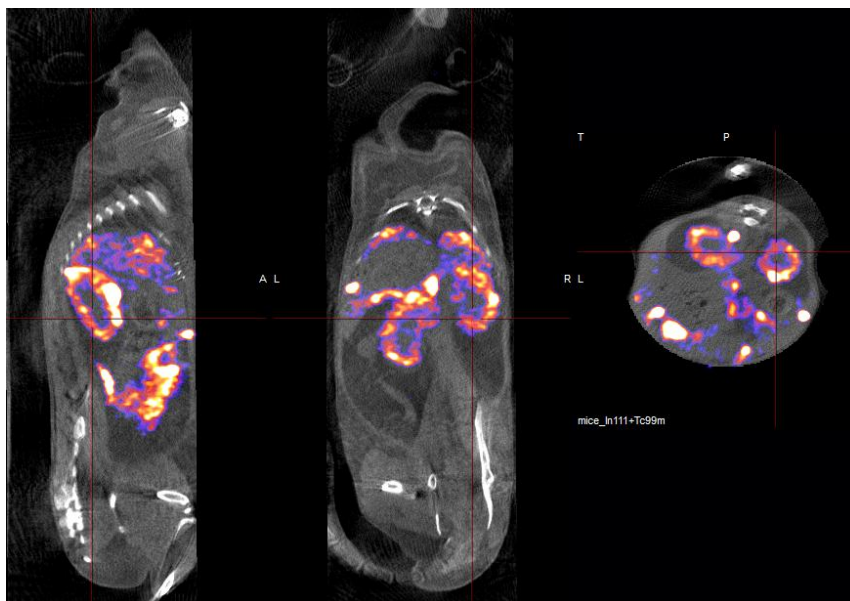

Figure 4.8. *This figure shows displays the kidney cortex uptake in a transversal (left), sagittal (middle) and coronal (right) image of a NMRI mouse injected with both* ^{111}*In-trastuzumab and* ^{99m}*Tc-Affibody. The kidney cortex can be seen in all three slices.*

Images of tissue samples taken with digital autoradiography (blue) along with corresponding samples stained with hematoxilin are displayed in figure 4.9. All images are 30 μm tissue samples of kidneys from NMRI mice from different injections. The top row shows a tissue sample from the same mouse injected with both radionuclides. Images 1 and 2 are the result of radionuclide separation with the IDL-software that was previously mentioned. As expected, ^{111}In-trastuzumab displays a more homogenous distribution, whilst ^{99m}Tc-Affibody seems to concentrate in the renal cortex in image 2.

The lower row consists of mice injected either trastuzumab or Affibody. These images did not undergo radionuclide separation. The same tendency is observed here; trastuzumab distributes somewhat evenly and Affibody is concentrated in the kidney cortex.
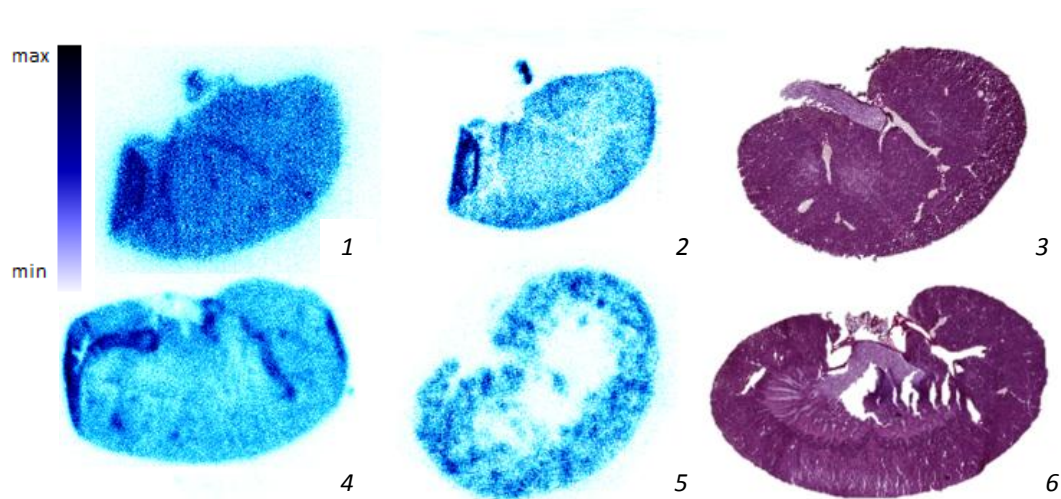

Figure 4.9 Results from digital autoradiography. *1*. ^{111}In-trastuzumab uptake in kidney 15 h.p.i. with radionuclide separation. *2*. ^{99m}Tc-Affibody uptake 6 h.p.i. with radionuclide separation. *3*. Tissue sample stained with hematoxilin *4*. ^{111}In-trastuzumab uptake 15 h.p.i. with no radionuclide separation. *5*. ^{99m}Tc-Affibody uptake 6 h.p.i. with no radionuclide separation *6*. Tissue sample stained with hematoxilin.

Comparison between the single- and dual radionuclide protocols for both the microSPECT and the gamma counter are displayed in table 4.1.

Table 4.1. Comparative biodistribtion of trastuzumab and Affibody in NMRI mice injected with both molecules. Data from 3 NMRI mice were used for the dual radionuclide measurements and data from 2 mice were used for the single-radionuclide measurements respectively. Affibody uptake is 6 h.p.i. and trastuzumab uptake is 15 h.p.i. Data presented as mean %IA/g. ND: not determined.

	microSPECT/CT				Gamma counter			
	Single protocol		**Dual protocol**		**Single protocol**		**Dual protocol**	
	[99m]Tc	[111]In	[99m]Tc	[111]In	[99m]Tc	[111]In	[99m]Tc	[111]In
Kidney	*11,8*	*ND*	*10,9*	*ND*	*16,1*	*ND*	*12,9*	*ND*
Liver	*ND*	*5*	*ND*	*9,2*	*ND*	*5,4*	*ND*	*9,0*

5 Discussion

In order to perform measurements using multiple radionuclides as a method of visualizing more than one molecule in the same animal at the same time, several considerations must be taken into account. The primary issues with multiple radionuclide imaging are the crosstalk between different energy windows and dead time. Dead time corrections are of special concern when measuring dual radionuclides, mainly because of different half-lives, but also due to varying uptake in different organs.

Phantom measurements

The SPECT/CT and scintillation counter systems correct for crosstalk contribution automatically. These functions were investigated by comparing their ability to quantitatively measure a single radionuclide against their capability of doing so when two radionuclides are measured simultaneously. For lower activities (4 kBq), the gamma counter underestimated ^{99m}Tc, which might seem counter-intuitive at first, since some down-spill in from ^{111}In in the ^{99m}Tc window is expected. In contrast, the scintillation counter overestimated ^{111}In. A possible reason for this is that, because of the high geometric efficiency of the scintillation counter, summation peaks from ^{99m}Tc and ^{111}In end up in the ^{111}In energy window. The 140,5 keV gamma photon from ^{99m}Tc and the 245,5 gamma photon from ^{111}In will, if they are registered as one count, end up in the ^{111}In energy window. Nevertheless, these results indicate a systematic error and no trends could be observed.

However, because of the dead time-related problems with the scintillation counter, it is important that these correction factors are derived from phantom measurements with activities matching those of an actual study. One such experiment was performed, were the dead times for each acquired data point were closer to those of the animal pilot study. Unlike the previous measurement, these results showed no constant deviation, but instead displayed clear trends. The initial overestimation of ^{99m}Tc is most likely due to down-spill contributions from ^{111}In. This would also explain the quick descent of the curve as the contribution from ^{111}In decreases. Since the dead time-factor is quite high, summation peaks are more likely to be a problem. This could explain the rising trend in the ^{111}In-curve as the amount of ^{99m}Tc increases. From these results one can draw the conclusion that curves for a larger array of activities must be acquired.

The SPECT measurements displayed deviations no larger than 6 percent, matching the accuracy of the scintillation counter at low activities. These results indicate that the dual-radionuclide protocol for the SPECT overestimates both radionuclides except for higher concentrations of ^{99m}Tc. At the moment however, more data points are needed before any definite conclusions can be made.

For low activities of ^{99m}Tc the Biomolex 700 imager highly overestimates ^{99m}Tc. This is because of lacking statistics; the radionuclide separation program will misread random fluctuations in the ^{111}In spectrum as well as instrument background as contributions from ^{99m}Tc. It is much more likely for ^{99m}Tc to end up in the second energy bin than for ^{111}In. Should the contribution from ^{99m}Tc be low enough, a certain amount of ^{111}In from this energy bin might be registered as ^{99m}Tc, leading to an overestimation. The effects should lessen with a new set of measurements; however, due to lack of time, no such measurement has yet taken place. The initial measuring times were quite short compared

to those used in the study, and from the results it is quite clear that the statistics of the phantom measurements should lie closer to those in the pilot animal study.

Pilot animal study

Previous animal studies investigating uptake and biodistribution of HER2-binding Affibody have shown high uptake in kidneys and bladder. This was confirmed by all three instruments utilizing dual-radionuclide protocols. The uptake in the renal cortex was, unlike previous studies utilizing clinical cameras, clearly visualized by the NanoSPECT/CT (figure 4.8). The high resolution of the NanoSPECT/CT might be advantageous in investigating the features of Affibody; the uptake in the mediastinal lymph nodes was unexpected and previous studies have not reported similar findings. A probable explanation for this is that clinical scanners were used during those studies and, having inferior spatial resolution compared to the camera used in this study, most likely could not visualize the uptake [23].

The first group of mice injected with ^{111}In-trastuzumab was injected intravenously through the tail vein. This proved difficult and not all injections were successful. This could have potentially degraded the picture quality. Because of these difficulties all future injections, both ^{111}In-trastuzumab and ^{99m}Tc-Affibody, were intraperitonial. Intraperitonial injections could further delay uptake of trastuzumab in mice, which also might have contributed to a lower contrast. This made it difficult to draw good ROI:s in the liver, where trastuzumab uptake is high. Because of this, it is difficult to draw any definite conclusions regarding the liver uptake. Even so, the dual-radionuclide protocol overestimated the uptake by several percent, mirroring the phantom experiments.

Quantification proved somewhat easier in this case since the kidneys were displayed in good contrast and had a clearly visible higher uptake in the cortex. This is largely due to Affibodys rapid kinetics which made it possible to perform acquisitions at a point in time when uptake was high. The main challenge and source to possible errors stems from InVivoScope inability to draw 3-dimensional ROI:s. Due to the inhomogeneous uptake in the kidneys, no mean value could be used and thus the kidney must be quantified in its entirety.

The scintillation counter overestimated ^{111}In-trastuzumab uptake and underestimates ^{99m}Tc-Affibody uptake. This was also seen in the phantom experiments and if corrections are made, the results are slightly better.

When examining the uptake in liver, there is little deviation between the two systems; both systems overestimate uptake by several percent when measuring with the dual-radionuclide protocol. The largest deviation can be found in the single-protocol measurements for kidneys, a somewhat surprising result as there were no problems with dead time with the scintillation counter in these measurements.

Imaging of tissue samples with the Biomolex 700 gave expected results, such as a higher uptake of ^{99m}Tc-Affibody in the renal cortex and a more homogenous distribution of trastuzumab. In the single-radionuclide measurement of ^{99m}Tc-Affibody it is possible to distinguish structures not seen in the dual-radionuclide measurement. These are most likely kidney glomeruli; a capillary structure which plays a part in the initial steps of the urine filtration process. As mentioned previously, these could not be seen in images that had undergone image separation. The reason for this is more likely to pertain to lacking

statistics rather than an error in radionuclide separation, since initial activities in dual-radionuclide tissue samples were low.

When performing dual-radionuclide imaging with mice, careful planning and preparations are necessary. Due to differences between instruments, half-life of radionuclides and biological uptake of the radiotracers, injection times and the amount of activity injected must be carefully planned. The importance of this was realized several times during the animal pilot study. Because all instruments have different activity intervals in which measuring is optimal, it is important to plan the amount of each injected radiotracer accordingly. Should ^{111}In-Trastuzumab uptake in liver be high enough for the count rate to cause dead time problems with the scintillation counter, it might not be possible to simultaneously with high accuracy quantify ^{99m}Tc-Affibody activity, because of the differences in half-life.

Future work

There are several conclusions that can be drawn from these experiments. Crucial to the accuracy of the end results in a study as comprehensive as this one is a solid foundation of thoroughly performed phantom measurements that can be used to correct for crosstalk and dead-time. The scintillation counter is extra sensitive to this, and more measurements are needed before correction factors can be estimated and put to use. This is not exclusive to dual-radionuclide measurements; studies utilizing a single radionuclide could benefit greatly from dead-time corrections as well, especially when long half-lives and time are important factors.

For best possible results, initial calibrations of the instruments should be based upon radionuclides whose activity has been predetermined with the highest accuracy possible. In this study, calibrations were based on samples whose activities were determined by instruments used for daily clinical use. This grants the equipment a certain dependability and reliability, but when dealing with activities around only a few kBq, a more accurate determination of activity of the calibration sources could be vital to the end results. Absolute calibration could therefore be considered a time consuming but necessary task.

6 Conclusion

This work has shown that it is possible to perform quantitative dual-radionuclide measurements on all systems used in this study. However, the advantages of imaging with several radionuclides simultaneously have to be weighed against the additional errors that are introduced in such measurements. Depending on the study it is possible that these uncertainties could be small compared to biological variations. Results from phantom studies suggest that corrections for dead-time and crosstalk can be made.

Acknowledgements

1. Pichler, B.J., H.F. Werhl, and M.S. Judenhofer, *Latest Advances in Molecular Imaging Instrumentation.* Journal of Nuclear Medicine, 2008. **48**.
2. Khalil, M.M., et al., *Molecular SPECT Imaging: An Overview.* Internation Journal of Molecular Imgaing, 2011. **2011**.
3. Franc, B.L., et al., *Small-Animal SPECT and SPECT/CT: Important Tools for Preclinical Investigation.* Journal of Nuclear Medicine, 2008. **49**(10): p. 1621-1663.
4. *Absorbed-Dose Specification In Nuclear Medicine.* Journal of the ICRU, 2002. **2**(1).
5. Figueiras, F.P., et al., *Simultaneous Dual-tracer PET Imaging of the Rat Brain and its Application in the Study of Cerebral Ischemi.* Molecular Imgaing and biology, 2010. **13**: p. 500-510.
6. M, M., et al., *Dynamic and Static Small-Animal SPECT in Rats for Monitoring Renal Function After 177Lu-Labeled Tyr3-Octreotate Radionuclide Therapy.* Journal of Nuclear Medicine, 2010. **51**: p. 1962-68.
7. Zhao, J., et al., *Determination of HER2 Gene Amplification by Chromogenic In Situ Hybridization (CISH) in Archival Breast Carcinoma.* Modern Pathology, 2002. **15**(6): p. 657-665.
8. L, S., et al., *Dual-labeled trastuzumab-based imaging agent for the detection of human epidermal growth factor receptor 2 overexpression in breast cancer.* Journal of Nuclear Medicine, 2007. **48**(9): p. 1501-10.
9. Baum, R.P., et al., *Molecular Imaging of HER2-Expressing Malignant Tumors in Breast Cancer Patients Using Synthetic 111In- or 68Ga-Labeled Affibody Molecules.* Journal of Nuclear Medicine, 2010. **51**(6): p. 892-897.
10. Perik, P.J., et al., *Indium-111–Labeled Trastuzumab Scintigraphy in Patients With Human Epidermal Growth Factor Receptor 2–Positive Metastatic Breast Cancer.* Journal of Clinical Oncology, 2006. **24**(15): p. 2276-2282.
11. Kagadis, G.C., et al., *In vivo small animal imaging: Current status and future prospects.* Medical Physics, 2010. **37**(12).
12. Kemp, R.A.d., et al., *Small-Animal Molecular Imaging Methods.* Journal of Nuclear Medicine, 2010. **51**: p. 185-325.
13. Nicolau Beckmann, et al., *In Vivo mouse imaging and spectroscopy in drug discover.* NMR in Medicine, 2007. **20**: p. 154-185.
14. Yarden, Y., *The EGRF family and its ligands in human cancer: signalling mechanisms and therapeutic opportunities.* European Journal of Cancer, 2001. **37**: p. 3-8.
15. Cobleigh, M.A., et al., *Multinational study of the efficacy and safety of humanized anti-HER2 monoclonal antibody in women who have HER2-overexpressing metastatic breast cancer that has progressed after chemotherapy for metastatic disease.* Journal of Clinical Oncology, 1999. **17**: p. 2639-48.
16. Rydén, L., et al., *Reproducibility of human epidermal growth factor receptor 2 analysis in primary breast cancer: a national survey performed at pathology departments in Sweden.* Acta Oncologica, 2009. **6**(48): p. 860-6.
17. DJ, V., et al., *Overexpression of the c-erb B-2 oncoprotein in human breast carcinomas: Immunohistological assessment correletaes with gene amplification.* The Lancet, 1987. **330**(8550): p. 69-72.
18. Tai, W., R. Mahato, and K. Cheng, *The role of HER2 in cancer therapy and targeted drug deliver.* Journal of Controlled Release, 2010. **146**: p. 264-275.
19. Goldenberg, M., *Trastuzumab, a recombinant DNA-derived humanized monoclonal antibody, a novel agent for the treatment of metastatic breast cancer.* Clinical Therapeutics, 1999. **21**(2): p. 309-318.
20. Philippe, L.B. and J.P.-G. Martine, *Current Paradigms for the Use of HER2-Targeted Therapy in Early-Stage Breast Cancer.* Clinical Breast Cancer, 2008. **8**: p. 157-165.
21. I, R. and Y. Y, *The Basic Biology of HER2.* Annals of Oncology, 2001(12): p. 3-7.

22.   Tran, T.A., et al., *Effects of Lysine-Containing Mercaptoacetyl-Based Chelators on the Biodistribtution of Tc-99m-labeled Anti-HER2 Affibody Molecules.* 2008(19): p. 2568-2576.
23.   Tran, T.A., et al., *Design, synthesis and biological evaluation of a multifunctional HER2-specfic Affibody molecule for molecular imaging.* Journal of Medical Molecular Imgaing.
24.   Marjolijn, H.N., et al., *Preclinical characterisation of 111In-DTPA-trastuzumab.* British Journal of Pharmacology, 2004(143): p. 99-106.